Available online at www.sciencedirect.com

ScienceDirect

Energy Procedia 44 (2014) 69 – 76

Energy Procedia

E-MRS Spring Meeting 2013 Symposium D - Advanced Inorganic Materials and Structures for Photovoltaics, 27-31 May 2013, Strasbourg, France

Influence of a thin contact underlayer on the Al incorporation in $CuIn_{1-x}Al_xSe_2$ films for photovoltaic applications

S. Martín* and C. Guillén

Departamento de Energía. Centro de Investigaciones Energéticas, Medioambientales y Tecnológicas (CIEMAT), Avda. Complutense, 40, Madrid, E-28040 (Spain)

Abstract

The influence of a thin metal underlayer on the chalcopyrite growth was studied. $CuInSe_2$ (CIS) and $CuIn_{1-x}Al_xSe_2$ (CIAS) thin films were grown by a two-stage process (stacked metal layers evaporation and subsequent selenisation) onto Mo and bared soda-lime glass substrates. Due to the difficulty found for get CIAS samples onto Mo, a thin Al layer was evaporated before the metallic stack destined to obtain CIS and CIAS films. This work shows the differences that appear between the CIS and CIAS samples evaporated onto both substrates, with and without the thin Al underlayer. By means of the characterisation of the samples, it has been observed that the use of Mo contact modifies the usual formation pathway of CIAS for the two-stage process. The evaporation of the thin Al layer on Mo promotes a higher grade of reaction of the CIAS phases.

Keywords: Chalcopyrite; Evaporation; Selenisation; CIAS; $Cu(In,Al)Se_2$; Mo; $MoSe_2$

* Corresponding author. Tel.: +34 913466679.
E-mail address: sofia.martin@ciemat.es

doi:10.1016/j.egypro.2013.12.011

1. Introduction

Chalcopyrites represent a very important group of semiconductors with significant applications in optoelectronic devices. In this regard, in the photovoltaic field, $CuIn_{1-x}Ga_xSe_2$ (CIGS) captures the maximum attention as a very suitable material for absorber layers in high-efficiency thin film solar cells [1, 2]. The results achieved with this CIS related material have presented however some limitations in high-Ga content CIGS devices [3]. As solution, the partial substitution of In by Al instead Ga (which leads to form $CuIn_{1-x}Al_xSe_2$) presents great advantages: this compound is much cheaper due to the abundance of Al, which does it less expensive than Ga and In. Besides, $CuIn_{1-x}Al_xSe_2$ (CIAS) covers a wider band gap than CIGS, from Eg=1.0 eV (corresponding to $CuInSe_2$) to Eg= 2.7 eV (corresponding to $CuAlSe_2$) [4], due to the different size of the atoms [3]. This wide range of band gap energies brings CIAS as an excellent candidate to be used in multi-junction solar cells [5]. For these reasons CIAS has been considered as a promising alternative. However it results necessary a deeper understanding of the reactions that take place during the formation of the compound and also the influence of the successive factors that conditions its growth to achieve the expected findings. Among these factors is the substrate on which the CIAS is grown. With the aim of know the maximum of the isolated layer under study, usually the CIAS is grown onto transparent and inert soda-lime glasses (SLG), which barely influence the preparation. But the presence of a back contact is indispensable for the solar cell device. Due to the requirements demanded for the back contact, as its behaviour as diffusion barrier for impurities from the substrate to the absorber, or good electronic properties allowing ohmic contact for the majority carriers at the interface and also low recombination rate for the minority carriers [6, 7], molybdenum is historically the metal chosen. However, it seems to complicate the growth of CIAS regarding to the use of SLG. This study tries to go deeper in the knowledge of the CIAS/Mo interaction toward CIAS formation, pointing to the idea that the Se reactions are which limits the complete CIAS formation. With this aim an Al interlayer has been evaporated between the Mo and the absorber layers. The systematic study of the films by means of optical, structural, compositional, electrical and morphological characterisation has been carried out to know the influence of the Mo back contact and also the Al interlayer on the CIAS preparation.

2. Experimental details

$CuInSe_2$ and $CuIn_{1-x}Al_xSe_2$ absorber layers were produced by selenisation of evaporated metallic precursors onto Mo-coated and bare soda-lime glass substrates. Mo back contact with thickness of 1.6 μm was deposited on SLG at room temperature with a planar DC magnetron sputtering system (Leybold type Z400) equipped with a Mo target of 99.9% purity. Power value of 106 W and working gas (Argon) pressure of 1.2 Pa were used in the preparation of the films. The evaporations of the absorber precursors were carried out in a single deposition system by e-beam evaporation of Cu and In and thermal evaporation of Al. The base pressure in the vacuum chamber was less than 10^{-4} Pa. The substrates were rotated during evaporation to promote good uniformity of the deposited layers.

In order to study the influence of a metal interlayer between the absorber and the substrate in the CIAS formation, an Al film of ~10 nm was evaporated onto Mo and glass substrates. CIS and CIAS precursors were subsequently evaporated onto the interlayer or the bare substrates. The individual layer thicknesses were controlled by quartz crystal microbalance monitoring and adjusted to obtain the desired metallic proportions. The precursors sequence used in the evaporation was (Al-interlayer)/In/Cu/In/(Al), according to satisfactory finds reported previously [8]. Due to the possible combinations, the thickness and atomic proportions of the samples are

Table 1. Average thickness of the samples selenised and Al/(Al+In) atomic ratio calculated.

	CIS	Al/CIS	CIAS	Al/CIAS
Thickness ±0.1 (μm)	0.8	0.8	0.9	1.0
Al/(Al+In) as-deposited	0.0	0.1	0.3	0.3

slightly different. The obtained values are included in Table 1. The precursor layers and elemental selenium were put together within a partially closed graphite box which was loaded in a quartz tube furnace for selenisation at 540ºC. Selenisation took place at 10^5 Pa under an Ar flux that remains constant throughout the process. The selenisation process was carried out in three steps as described in previous works [9, 10].

The optical transmittance (T) and total reflectance (R) of the samples were measured with a Perkin–Elmer LAMBDA 9 double beam spectrophotometer with integrating sphere in the 300-1800 nm wavelength range at room temperature, taking the air as reference. The thickness of the films was obtained by means of a DEKTAK 3030 profilometer. The chemical composition was determined by energy dispersive analysis of X-ray (EDX) with an Oxford Instruments X-Max detector with a resolution of 124 eV. The surface morphology was examined by a Hitachi SU-6600 Scanning Electron Microscope (SEM) and the structural characterization was carried out by means of X-ray Diffraction (XRD) using a PHILIPS X'PERT diffractometer with CuK_α (λ= 1.54056 Å) radiation. Peak diffraction angles in the XRD patterns were converted to interplanar d-spacings and thus, phase identification has been carried out by comparison of the observed d-spacing with the Joint Committee on Powder Diffraction Standards (JCPDS). To verify the type of electrical contact of the films with the Mo layer, I-V curves have been measured using a data acquisition program in the LabVIEW environment, at room temperature.

3. Results and discussion

The crystalline structure of the CIS and CIAS selenised samples onto both bare and Mo-coated glass substrates was characterised by XRD. Since no JCPDS standard files are available for $CuIn_{1-x}Al_xSe_2$, $CuInSe_2$ [11] and $CuAlSe_2$ [12] standards were used to identify the formation of CIAS according to Vegard's law, with a linear variation in lattice spacing as a function of x.

Fig. 1a shows the XRD patterns of CIS layers grown onto SLG and SLG/Mo. The presence of the main peaks (112), (204)/(220), (312)/(116) and (400) together with the smaller ones (101), (103) and (211), all marked in the graph with black dots, indicates the chalcopyrite structure of both films. The XRD pattern of the CIS sample grown on Mo layer shows in addition crystalline phases related with this element: peaks corresponding to Mo with bcc structure (110) and (200) [13] are identified, as well as (111) and (002) corresponding to fcc structure [14], that remain from the as-deposited Mo and are marked in the graph with asterisks. Furthermore in the figure the (100) and (110) reflections of $MoSe_2$ are appreciated [15]. The absence of $MoSe_2$ (00n) reflections suggests that the c-

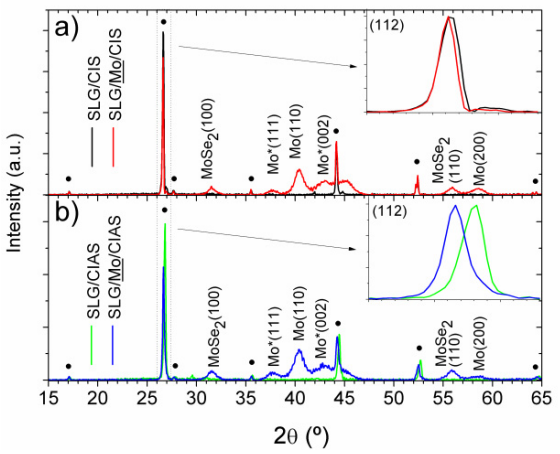

Fig. 1 XRD patterns of (a) CIS and (b) CIAS samples grown directly onto SLG and SLG/Mo substrates. Black dots identify the position of the peaks of the chalcopyrite structure. The insets show a zoom of the main (112) chalcopyrite peaks.

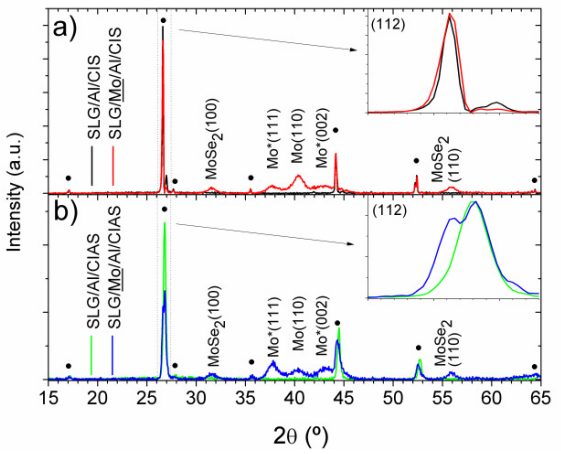

Fig. 2 XRD patterns of (a) CIS and (b) CIAS samples grown with an Al interlayer between the absorber and the substrates (SLG and SLG/Mo). Black dots identify the position of the peaks of the chalcopyrite structure.

axis of the $MoSe_2$ layer is parallel to the Mo surface which is known to promote good adhesion between the absorber and Mo [16]. XRD patterns of CIAS layers onto both substrates are depicted in Fig.1b. It is observed that the patterns are similar to those corresponding to CIS exhibited on top. The main differences that appear onto both substrates, among CIS and CIAS patterns, are detected by analysing what happens with the displacement of the main peak (112), since it is the range of angles where the reflection peaks have higher counts and so the analysis is simpler, plotted in the corresponding inset of Fig. 1a and Fig. 1b. In the top inset it is observed that the main CIS peak remains in the same position for the samples evaporated onto both substrates, although onto Mo the peak is slightly narrower. However in CIAS layers a big difference appears between the samples converted onto SLG and SLG/Mo: while onto bare glass the main peak undergoes a noticeable displacement toward higher angles, which indicates an Al incorporation corresponding to x= 0.2 in the chalcopyrite structure according to Vegard's law, the peak (112) of the sample evaporated onto SLG/Mo remains in the same angular position than the corresponding to CIS. This peak also shows several shoulders, indicating phases with a range of Al incorporation. This lack of displacement in the peaks of the CIAS layers evaporated onto Mo has been observed on numerous experiments in the laboratory under these same conditions. Due to the fact that evaporation and selenisation processes were exactly the same for the samples grown onto both substrates, one of the explanations that best fits these experimental results is that the cause of the differences is related to a modification of the selenisation process of the absorber, being this change promoted by the presence of the Mo layer.

With the aim of solve this problem, and according to previous works as the carried out by Marsillac et al. [17] and Perng et al [18] that modified the Mo/absorber interface in different ways, a thin Al layer was evaporated between Mo and the absorber layers. The thickness chosen for this interlayer, ~10 nm, was calculated to be much lower than that for the evaporated film intended for the CIAS formation. Its contribution to the sample only represents an Al ratio of x=0.02. To complete the comparison, this thin Al film was evaporated also onto the bare glass. The XRD patterns of these new samples, all of them with the Al interlayer between the substrate and the absorber layers, are depicted in Fig. 2, analogously to Fig. 1. As it can be seen, the full spectra of all the samples (with and without the Al interlayer) do not show great differences regarding to the chalcopyrite structure. However, concerning to Mo, differences appear in the spectrum of Mo bcc, since the peak Mo (110) lowers its intensity and Mo (200) disappears. This fact indicates that the Al interlayer has an effect in the way as the Mo reacts. The analysis of the main peak (112) of the chalcopyrite structure, shown in the insets of Fig. 2, reveals also noticeable differences. In CIS samples (Fig. 2a), the peak is located in the same angular position that the observed for the samples without the Al interlayer (Fig. 1a). However, a small peak is discerned at higher angle in the sample evaporated onto SLG, with the Al interlayer. This suggests that onto this substrate the Al interlayer has been incorporated in the CIS matrix, probably and due to its low proportion, only in some atomic layers, giving a

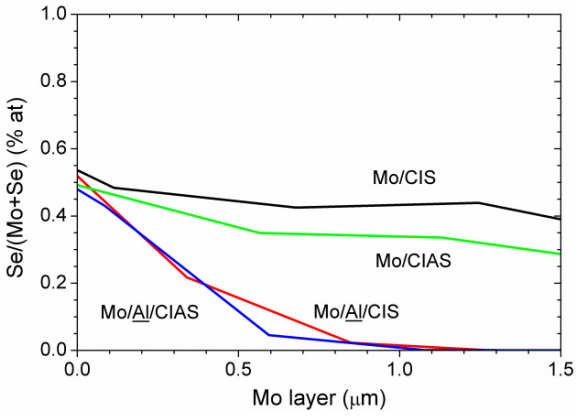

Fig. 3 Composition profile of the atomic ratio Se/(Se+Mo) along the Mo from the absorber/Mo to the Mo/SLG interfaces.

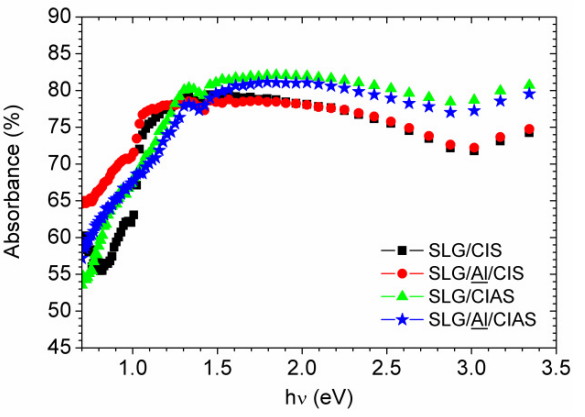

Fig. 4 Absorbance spectra of the samples grown onto glass

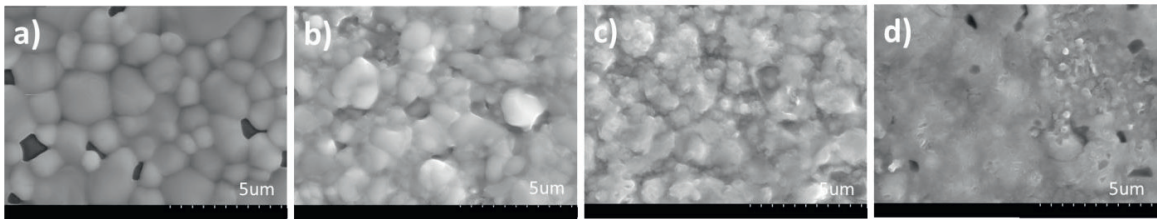

Fig. 5 SEM images of samples grown onto glass (a) SLG/CIS, (b) SLG/Al/CIS, (c) SLG/CIAS and (d) SLG/Al/CIAS

CIAS peak with low crystallinity but with a x=0.3, higher than the expected from the overall Al content. This behaviour is not observed in the CIS sample onto Mo. By means of the analysis of (112) peaks of CIAS samples with the Al interlayer, depicted in the inset of Fig. 2b, it is discerned that, onto SLG, this interlayer produces a widening on the main peak, centered at a position corresponding to x=0.2. Onto Mo a big difference is perceived with respect to that obtained without the Al interlayer: the presence of two well differentiated peaks, pointing a more complete incorporation of Al in CIS matrix with respect to the analogous sample without the Al back layer. Therefore, the addition of an Al interlayer between the substrate and the absorber promotes a better reaction to achieve CIAS formation. This effect seems to be stimulated by the selenisation of the Al layer situated next to the substrate.

It has been carried out a composition analysis along the transversal section in the samples grown onto Mo. The transversal section zone corresponding to the Mo layer is depicted in Fig. 3. In this figure it can be seen the evolution of the atomic ratio Se/(Mo+Se) in function of the depth where the data have been taken from the absorber/Mo interface toward the Mo/glass interface. It is observed in the graph noticeable differences among the samples deposited with the Al interlayer and the samples deposited directly onto the substrates. All of them have the same atomic ratio in the absorber/Mo interface probably related to the $MoSe_2$ layer [19]. However, as the analysis is performed in deeper points, the atomic ratio between both elements decreases to approximately 0% with the presence of the Al interlayer. The absence of the interlayer makes that the proportions remain constant with depth. Nevertheless, due to the similar intensity of the $MoSe_2$ related peaks detected in the XRD spectra of all the samples, this proportion does not necessarily indicate a wider $MoSe_2$ layer [20], since probably the elements have not completely reacted. This suggests that the Al interlayer reduces the penetration of Se into the Mo layer.
With the aim of confirm the structural results, optical characterisation has been performed for the samples. By means of the transmission and reflection spectra of the samples grown onto SLG, the absorbance coefficient has been calculated according to the equation A(%)=100-T(%)-R(%). This parameter represented as function of the energy of the incident photons in Fig. 4 provides an easy way to know where the absorption edge of the compounds is located. It can be observed that the obtained curves, depicted in Fig. 4, are in agreement with the XRD results. CIAS samples show a displacement of the edge to about 1.2 eV regarding to CIS samples, located in an energy corresponding to 1.0 eV. CIAS samples with and without Al interlayer exhibit a similar performance, however the Al interlayer modifies the behaviour of the optical properties at the energies lower than the absorption

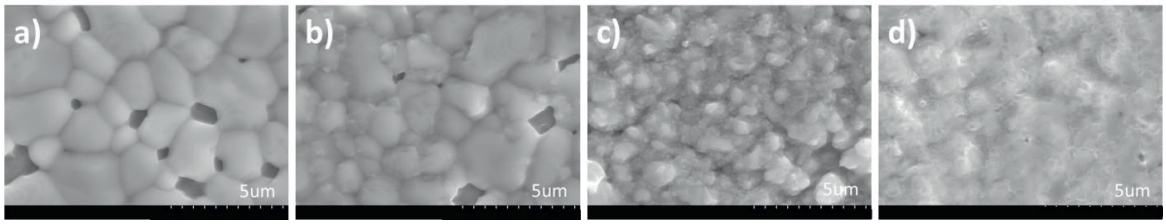

Fig. 6 SEM images of samples grown onto Mo (a) SLG/Mo/CIS, (b) SLG/ Mo/Al/CIS, (c) SLG/ Mo/CIAS and (d) SLG/ Mo/Al/CIAS

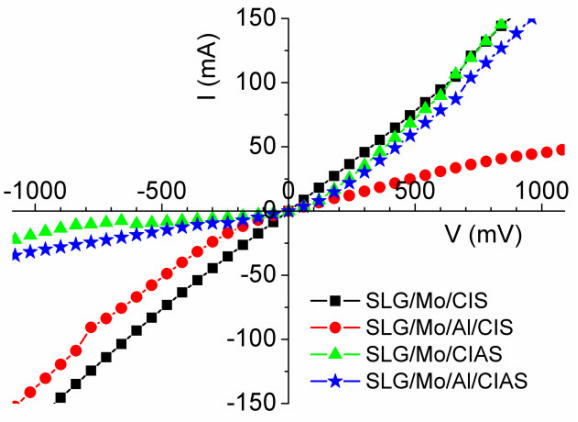

Fig. 7 I-V dark curves for the samples deposited onto SLG/Mo

edge: the sample with the Al interlayer shows higher absorption in this region, which implies the presence of absorbent phases not corresponding to CIS, probably related with a not complete Al incorporation in CIS matrix or its presence as aggregates. The reflectance spectrum has been taken for the samples onto Mo (not shown). It is observed that CIS samples exhibit a marked edge, while CIAS samples present a less sharp edge, which indicates the gradual Al incorporation.

SEM images of the film surface of the samples grown onto SLG and Mo are shown in Fig. 5 and Fig. 6 respectively. In those it is observed the morphological evolution of the films with the addition of Al , where it is appreciated a similar performance of the thin films onto the different substrates. All the layers show a homogeneous morphology across the surface. The images taken for CIS and CIAS samples without the Al interlayer, illustrated in Fig. 5a-6a and Fig. 5c-6c respectively, are consistent with previous works [3, 21], showing irregular conglomerates with grain coalescence higher for the CIS grains. By means of the comparison with the samples deposited onto the Al interlayer (Fig. 5b-6b and 5d-6d) it is concluded that the presence of Al as interlayer seems to generate some disorder during the growth, which is spread up to the surface.

I-V measurements depicted in Fig. 7 have been performed at room temperature for the CIS and CIAS thin films grown onto Mo, with and without the Al interlayer. It is observed that CIS sample presents an ohmic contact in the CIS/Mo interface that is related to the presence of $MoSe_2$ layer [19]. However, according to the curves plotted in the figure, the addition of Al leads to a rectifying behaviour with some increase of the contact resistance that is not desirable. Due to the work function is lower for Al than for Mo [22], the presence of the Al outside the CIS matrix makes that the junction between both layers rectifies. The fact that in the CIS sample with Al interlayer the maximum Al content is next to the surface, while in the CIAS samples it is more distributed along the layer, could explain the opposite senses of the rectifying contacts that can be observed in the figure.

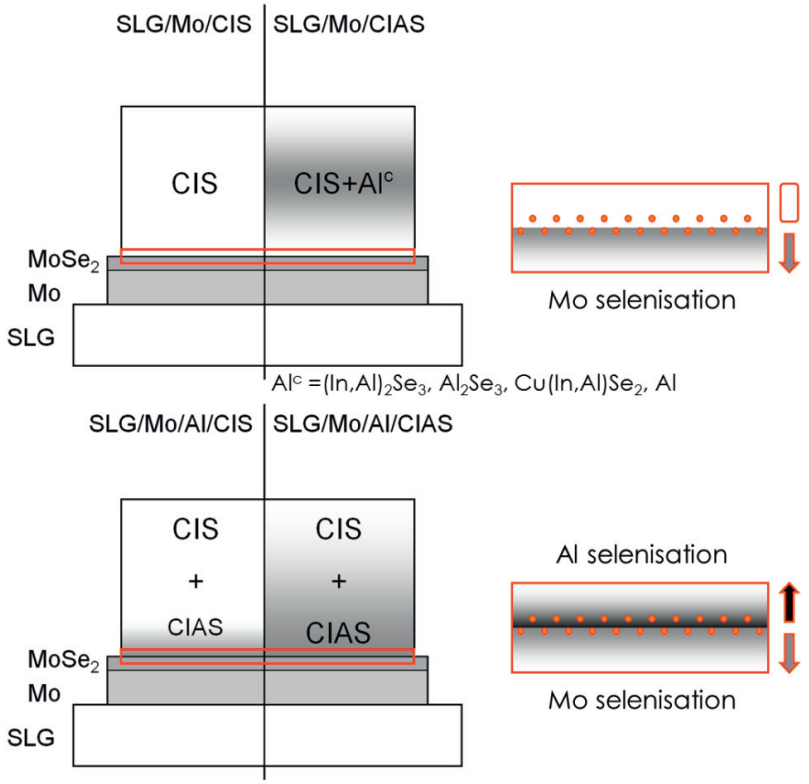

Fig. 8 Schematic model visualising the final scenarios of the different layers onto Mo. On top, in absence of the Al interlayer, CIS formation is completed but not the quaternary CIAS, with other Al compounds (Al^c) distributed along the layer. On bottom, with Al interlayer, the accumulation of Al on the Mo-side forces the selenisation, promoting the formation of CIAS phases. In the corresponding amplified pictures, the suggested situation for the absorber/Mo interface is depicted, where the Al interlayer reduces the penetration of Se into the Mo layer.

The findings discussed previously are summarised schematically in Fig. 8 for the samples grown onto Mo. The shown results point to the fact that the CIAS formation depends in great form on the substrate where the layer is grown. The information obtained from the structural analysis reflects that while CIS does not show impediments in the growth onto Mo, the presence of this layer complicates the formation of CIAS phases with reasonable crystallinity. From this it is deduced that the differences detected in the absorbers lie in the fact that the chemical activity of Se is distinct with both substrates since the formation of the semiconductor takes place via metal-selenides, implying differences in the absorber formation. The use of SLG as substrate does not seem to affect the growth of the absorber regarding to the Al incorporation and complete formation of the CIAS. In this case, according to previous studies [10], the Se captured by the sample is consumed firstly in the CIS formation which starts right after the melting point of selenium. Subsequently, from a temperature around 425ºC [23] the selenium begins to react with In-Al alloys, being necessary to reach temperatures near 480ºC to form the quaternary [3]. The annealing to higher temperatures leads to further reaction between these phases, although some Al remains out of the matrix as it is deduced from the structural and electrical properties of the samples. The use of Mo as substrate to the growth modifies this pathway of formation, since the Se existent in the sample is able to react and mix easily also with this element. The consumption of Se by Mo intended the $MoSe_2$ formation has been reported from temperatures below 400ºC completing the formation around 470ºC [20, 24]. For this reason the reaction between Mo and Se is thermodynamically preferred to that for Al and Se, which complicates the Al selenisation

due to the lowest availability of selenium that remains in the layer. From the results obtained by the structural and in-depth compositional analyses, it is observed that the Al interlayer on Mo promotes CIAS formation: Due to the trend of Al towards the bottom of the layer, it can be supposed that the Al interlayer will remain close to Mo side, which will produce an accumulation of the element in this region that will change the reactivity of Se with Mo. The formation of a CIAS phase during the CIS growth with Al interlayer as well as the composition profiles prove it. It is deduced that exists a competition among the Al and Mo selenisation processes, which complicates the Se spread into Mo by means of the Al selenisation. This promotes the formation of CIAS phases with high Al content that leads the formation of other phases and their interdiffusion toward a more homogeneous system. Furthermore this process does not block the formation of some $MoSe_2$, beneficial for a low resistance contact.

4. Conclusions

The results obtained from this study converge in the idea that the use of Mo contact complicates the usual formation pathway of CIAS for the two-stage process followed in this work. It has been found that the deposition of an Al interlayer seems to solve in part this problem,. The configuration used in the precursors stack, that led to good results in the growth of CIAS onto glass, does not work properly onto Mo. Therefore further studies are necessary in order to a better comprehension of the behaviour of the Se which plays an important role in the absorber formation.

Acknowledgements

This work has been supported by the Spanish Ministry of Economy and Competitiveness through the CIEMAT Photovoltaic Program. S. Martín should also thank to CIEMAT for the award of a PhD research fellowship.

References

[1] I. Repins, M.A. Contreras, B. Egaas, C. DeHart, J. Scharf, C.L. Perkins, B. To, R. Noufi, Prog. Photovol: Res. Appl. 16/3 (2008) 235.
[2] M.A. Green, K. Emery, Y. Hishikawa, W. Warta, Prog. Photovol: Res. Appl. 16/1 (2008) 61.
[3] D. Dwyer, I. Repins, H. Efstathiadis, P. Haldar, Sol. Energy Mater. Sol. Cells 94/3 (2010) 598.
[4] P.D. Paulson, M.W. Haimbodi, S. Marsillac, R.W. Birkmire, W.N. Shafarman, J. Appl. Phys. 91/12 (2002) 10153.
[5] Y.B.K. Reddy, V.S. Raja, B. Sreedhar, J. Phys. D: Appl. Phys. 39/24 (2006) 5124.
[6] K. Orgassa, H.W. Schock, J.H. Werner, Thin Solid Films 431-432/0 (2003) 387.
[7] M. Bär, L. Weinhardt, C. Heske, S. Nishiwaki, W.N. Shafarman, Physical Review B 78/7 (2008) 075404.
[8] S. Martín, G. Zoppi, R. Aninat, I. Forbes, C. Guillén, Mater. Chem. Phys. 140/1 236.
[9] R. Caballero, C. Guillén, Sol. Energy Mater. Sol. Cells 86/1 (2005) 1.
[10] S. Martín, C. Guillén, J. Cryst. Growth 336/1 (2011) 82.
[11] Joint Committee on Powder Diffraction Standards (JCPDS), file number 00-40-1487 for $CuInSe_2$.
[12] Joint Committee on Powder Diffraction Standards (JCPDS), file number 00-44-1269 for $CuAlSe_2$.
[13] Joint Committee on Powder Diffraction Standards (JCPDS), file number 00-042-1120 for Mo bcc
[14] Joint Committee on Powder Diffraction Standards (JCPDS), file number 96-900-8475 for Mo fcc.
[15] Joint Committee on Powder Diffraction Standards (JCPDS), file number 00-77-1715 for $MoSe_2$.
[16] D. Abou-Ras, C.T. Koch, V. Küstner, P.A. van Aken, U. Jahn, M.A. Contreras, R. Caballero, C.A. Kaufmann, R. Scheer, T. Unold, H.W. Schock, Thin Solid Films 517/7 (2009) 2545.
[17] S. Marsillac, P.D. Paulson, M.W. Haimbodi, R.W. Birkmire, W.N. Shafarman, Appl. Phys. Lett. 81/7 (2002) 1350.
[18] D.-C. Perng, J.-W. Chen, C.-J. Wu, Sol. Energy Mater. Sol. Cells 95/1 (2011) 257.
[19] T. Wada, N. Kohara, S. Nishiwaki, T. Negami, Thin Solid Films 387/1-2 (2001) 118.
[20] J. Koo, S. Jeon, M. Oh, H.-i. Cho, C. Son, W.K. Kim, Thin Solid Films 535/0 148.
[21] J. López-García, C. Guillén, Thin Solid Films 517/7 (2009) 2240.
[22] H.L. Skriver, N.M. Rosengaard, Physical Review B 46/11 (1992) 7157.
[23] S. Jost, F. Hergert, R. Hock, M. Purwins, R. Enderle, phys. stat. sol (a) 203/11 (2006) 2581.
[24] S. Lee, J. Koo, S. Kim, S.-H. Kim, T. Cheon, J.S. Oh, S.J. Kim, W.K. Kim, Thin Solid Films 535/0 206.